

# Chromatic Transition of Polydiacetylene in Solution

BENJAMIN CHU\*

Chemistry Department, State University of New York at Stony Brook, Long Island, New York 11794-3400

RENLIANG XU†

Chemistry Department, University of Toronto, Toronto, Ontario M5S 1A1, Canada

Received April 9, 1991 (Revised Manuscript Received October 14, 1991)

Polydiacetylenes,  $(=CRC=CCR'=)_n$ , consisting of polydiacetylene and its derivatives, are prototype conducting polymers.<sup>1</sup> Most polydiacetylenes are insoluble even in exotic solvents and are infusible because of their rotation-restricted stiff backbone.<sup>2</sup> *Pn*BCMU polymers in which  $R' = R = (CH_2)_n OCONHCH_2COO(CH_2)_3CH_3$  with  $n = 3$  and 4, and customarily known as P3BCMU and P4BCMU, respectively, were synthesized about a decade ago.<sup>3</sup> There have been extensive studies on the electronic, mechanical, optical, and conformational properties of polydiacetylenes in both the solid state (crystals and thin films) and the liquid state (gels and solution). Conducting polymers, in particular polydiacetylene, have been the subject of several books.<sup>4-7</sup>

Polydiacetylenes have many interesting properties, such as the large quasi-one-dimensional structure of their single crystals, high third-order optical susceptibility, large optical nonlinearity, and high photoconductivity.<sup>8-10</sup> One dramatic but controversial property to which most attention has been paid and which we want to discuss in this Account is the peculiar color change of polydiacetylenes in solution. The nature of the color change of polydiacetylenes in solution also reflects the color change property in the solid state. The color change of polydiacetylenes can be used to monitor any one of the ambient parameters, such as time-temperature exposure, pressure, radiation exposure, gas exposure, pH, and humidity. Commercial products include the development of a diacetylene ink that can be used to print a bar-code label that acts as a time-temperature or radiation dosage indicator from the color change.<sup>11,12</sup> This bar code can be used not only to provide for static information related to automatic product identification and pricing in merchandising but also to function as an automated dosimetry system.

Benjamin Chu was born in Shanghai, China, and is now Leading Professor of Chemistry at SUNY Stony Brook. He received his B.Sc., magna cum laude, from St. Norbert College in 1955 and his Ph.D. in physical chemistry (with Richard M. Diamond) from Cornell University in 1959. Following a postdoctoral appointment with Peter J. W. Debye (1958-1962), he was appointed Assistant Professor of Chemistry at the University of Kansas. He moved to SUNY Stony Brook in 1968 as Professor of Chemistry. He was an Alfred P. Sloan Fellow (1966-1968), a Guggenheim Fellow (1968-1969), a JSPS Visiting Professor (1975-1976), and a Humboldt Awardee (1976-1977). His research interests in polymers, colloids, and biophysics include laser light scattering, synchrotron X-ray scattering, structure and dynamics of polymer solutions and blends, polymer colloids, ionomers, and polyelectrolytes as well as DNA gel electrophoresis.

Renliang Xu was born in the People's Republic of China and has been a postdoctoral awardee from the National Sciences and Engineering Research Council of Canada at the University of Toronto. He received his B.Sc. from Fudan University in 1982 and his Ph.D. in physical chemistry from SUNY Stony Brook in 1988. He was a postdoctoral associate with Mitchell A. Winnik in Toronto. His research interests are laser light scattering, conducting polymers, and polymer colloids.

The chromatic transitions exhibited by solutions of soluble polydiacetylenes can be induced by changes in either temperature or solvent quality.<sup>13-18</sup> For example, solutions of P4BCMU in toluene at room temperature are red and will turn yellow either by adding chloroform (a good solvent) or by raising the temperature. It has been proposed that the color change from yellow to red is intimately related to a corresponding conformational change from coil (yellow) to rod-like (red) chain. At the heart of the debate is a fundamental question concerning the nature of the transition: Is the chromatic transition driven purely by an intramolecular effect, the so-called single-chain coil-to-rod transition, or by an intermolecular effect which results in the formation of aggregates of polydiacetylene chains? On the basis of light scattering<sup>19</sup> and electric birefringence data,<sup>20,21</sup> the single-chain coil-to-rod transition hypothesis postulates

\* Author to whom all correspondence should be addressed.

† Present address: Coulter Corporation, Hialeah, FL 33010.

(1) Matsuda, H.; Nakanishi, H.; Kato, S.; Kato, M. *J. Polym. Sci., Polym. Chem. Ed.* **1987**, *25*, 1663-1669.

(2) Baughman, R. H.; Chance, R. R. *J. Polym. Sci., Polym. Phys. Ed.* **1976**, *14*, 2037-2045.

(3) Patel, G. N. *Polym. Prepr. (Am. Chem. Soc., Div. Polym. Chem.)* **1978**, *19*, 154-159.

(4) *Nonlinear Optical Properties of Organic Polymeric Materials*; Williams, D. J., Ed.; ACS Symposium Series 233; American Chemical Society: Washington, DC, 1983. *Crystallography of Ordered Polymers*; Sandman, D. J., Ed.; ACS Symposium Series 337; American Chemical Society: Washington, DC, 1987.

(5) *Polydiacetylene*; Bloor, D., Chance, R. R., Eds.; NATO Advanced Science Institutes Series E: Applied Science; Martinus Nijhoff Publishers: Dordrecht, The Netherlands, 1985; Vol. 102.

(6) *Advanced Nonlinear Polymer Inorganic Crystallography Liquid Crystallography, Laser Media*; Musikant, S., Ed.; Proceedings of SPIE—The International Society of Optical Engineering; SPIE: Bellingham, WA, 1988; Vol. 824.

(7) *Synthetic Metals*; Heeger, A. J., Ed.; Proceedings of the International Conference on the Science and Technology of Synthetic Metals; Elsevier: Sequoia, The Netherlands, 1987; Vol. 18, pp 1-3.

(8) Marrian, C. R. K.; Colton, R. J.; Snow, A.; Taylor, C. J. *Mater. Res. Soc. Symp. Proc.* **1987**, *76*, 353-357.

(9) Korshak, Y. V.; Medvedeva, T. V.; Ovchinnikov, A. A.; Spektor, V. N. *Nature (London)* **1987**, *326*, 370-372.

(10) Shutt, J. D.; Rickert, S. E. *Langmuir* **1987**, *3*, 460-467.

(11) Baughman, R.; Chance, R. R. *Polym. Prepr. (Am. Chem. Soc., Div. Polym. Chem.)* **1986**, *27*, 67-68.

(12) Prusik, T.; Montesalvo, M.; Wallace, T. *Radiat. Phys. Chem.* **1988**, *31*, 441-447.

(13) Patel, G. N.; Chance, R. R.; Witt, R. D. *J. Chem. Phys.* **1979**, *70*, 4387-4392.

(14) Lim, K. C.; Fincher, C. R.; Heeger, A. J. *Phys. Rev. Lett.* **1983**, *50*, 1934-1937.

(15) Lim, K. C.; Sinclair, M.; Casalnuovo, S. A.; Fincher, C. R.; Wudl, F.; Heeger, A. J. *Mol. Cryst. Liq. Cryst.* **1984**, *105*, 329-352.

(16) Berlinsky, A. J.; Wudl, F.; Lim, K. C.; Fincher, C. R.; Heeger, A. J. *J. Polym. Sci., Polym. Phys. Ed.* **1984**, *22*, 847-852.

(17) Casalnuovo, S. A.; Lim, K. C.; Heeger, A. J. *Makromol. Chem., Rapid Commun.* **1984**, *5*, 77-81.

(18) Chance, R. R.; Sowa, J. M.; Eckhardt, H.; Schlott, M. *J. Phys. Chem.* **1986**, *90*, 3031-3033.

(19) Lim, K. C.; Heeger, A. J. *J. Chem. Phys.* **1985**, *82*, 522-530.

Table I  
P4BCMU Solution Properties

solvent	technique	remarks	ref
CHCl <sub>3</sub> (good solvent)	FTIR, ABS	phase diagram	25
<i>n</i> -C <sub>6</sub> H <sub>14</sub>		color change	
MEK (>60 °C)	DSC, Δ <i>H</i>	planar structure	26
<i>m</i> -xylene (>95 °C)			
acetic acid (>45 °C)			
CHCl <sub>3</sub> /C <sub>6</sub> H <sub>14</sub>	DLS, ABS	single chain	19–21
toluene (>70 °C, good solvent)	TEB	rod-to-coil transition	
toluene	(∂ <i>n</i> /∂ <i>C</i> ) <sub>T,P</sub> , DLS	rod aggregates	22–24
CHCl <sub>3</sub>	Raman	(∂ <i>n</i> /∂ <i>C</i> ) <sub>T,P</sub> same for rod/coil	
THF/toluene	DLS, ABS, η, EM	semidilute aggregates	27
	SAXS	rod-like aggregates	39
toluene	LS, SANS	rod aggregates	28
DMF			
toluene	TEB, DLS	neutral coil	29–31
CHCl <sub>3</sub> /C <sub>6</sub> H <sub>14</sub>	ABS, EP	charged rod	
CHCl <sub>3</sub>			
bromoform	IR, ABS, SANS	chain-stiffness increases with side-group interactions	32
CHCl <sub>3</sub>	flow birefringence	birefringence in semidilute solution	33
toluene/CHCl <sub>3</sub>	CM	single-chain rod-to-coil transition	34
toluene- <i>d</i> <sub>8</sub> , COCl <sub>2</sub>	<sup>13</sup> C NMR, DSC	solution/solid state thermochromatic transition from strain on the backbone by side chains	35
toluene	SAXS	ribbon-like aggregates	36

that aggregation occurs subsequent to the single-chain coil-to-rod transition and is a consequence of intermolecular aggregation by the already extended rod-like polydiacetylene chains. In the intermolecular hypothesis<sup>22–24</sup> the color change involves the aggregation of polymer chains or segments which form a fringed micelle-like structure consisting of many polymer chains or segments. The aggregation process forces the polymer chains together, resulting in the formation of extended rod-like polymer chains or segments which cause the color change. Simply stated, the debate is similar to the chicken or egg argument: Which comes first, the chicken or the egg? So, in the polydiacetylene chromatic transition, we ask the question: Do the polymer chains straighten out first before they aggregate? Or do they aggregate and straighten out in the process? We shall present the experimental evidence which tries to clarify some problems associated with this controversy. We do not claim that we have resolved all the disagreements. Our viewpoint is necessarily subjective.

### Brief Review of Existing Experiments

Polydiacetylenes, especially P4BCMU, have been studied with a very extensive list of physical techniques including nuclear magnetic resonance (<sup>13</sup>C NMR), Fourier transform infrared spectroscopy (FTIR), transient electric birefringence (TEB), dynamic light scattering (DLS), static light scattering (SLS), Raman scattering, absorption spectroscopy (ABS), differential scanning calorimetry (DSC), viscosimetry (η), refractive index increment (∂*n*/∂*C*)<sub>T,P</sub>, electron microscopy (EM), small angle X-ray scattering (SAXS), small angle neutron scattering (SANS), electrophoresis (EP), and Cotton-Mouton measurements (CM). Table I lists

(20) Lim, K. C.; Kapitulnik, A.; Zacher, R.; Heeger, A. J. *J. Chem. Phys.* **1985**, *82*, 516–521.

(21) Lim, K. C.; Kapitulnik, A.; Zacher, R.; Heeger, A. J. *J. Chem. Phys.* **1986**, *84*, 1058–1059.

(22) Wenz, G.; Muller, M. A.; Schmidt, M.; Wegner, G. *Macromolecules* **1984**, *17*, 837–850.

(23) Muller, M. A.; Schmidt, M.; Wegner, G. *Makromol. Chem., Rapid Commun.* **1984**, *5*, 83–88.

(24) Schmidt, M.; Wegner, G. *J. Chem. Phys.* **1986**, *84*, 1057–1058.

(25) Patel, G. N.; Chance, R. R.; Witt, J. D. *J. Chem. Phys.* **1979**, *70*, 4387–4392.

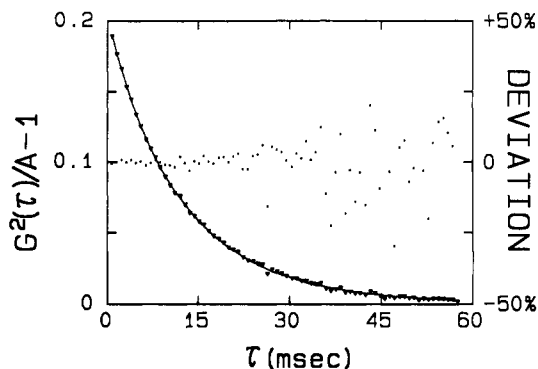


Figure 1. Net intensity-intensity time correlation function (inverted triangles) of P4BCMU with  $M_w = 2.4 \times 10^6$  g/mol in toluene,  $C = 1 \times 10^{-6}$  g/g, and the fitted curve from CONTIN (solid line) with the relative deviation [(data<sub>measd</sub> - data<sub>calcd</sub>)/data<sub>measd</sub>]. The corresponding distribution (solid line) is shown in Figure 2. Reprinted with permission from ref 29. Copyright 1989 American Chemical Society.

some of the conclusions and references for experiments performed on P4BCMU solutions so far. The conflict between the two models appears to persist. On the basis of the same data, we shall first summarize the accepted conclusions.

### Yellow Neutral Coils and Red Charged Rod Aggregates

The conformation of soluble P4BCMU in a good solvent, such as chloroform, has been found to be neu-

(26) Patel, G. N.; Witt, J. D.; Khanna, Y. P. *J. Polym. Sci., Polym. Phys. Ed.* **1980**, *18*, 1383–1391.

(27) Peiffer, D. G.; Chung, T. C.; Schulz, D. N.; Agarwal, P. K.; Garner, R. T.; Kim, M. W. *J. Chem. Phys.* **1986**, *85*, 4712–4718.

(28) Rawiso, M.; Aime, J. P.; Fave, J. L.; Schott, M.; Muller, M. A.; Schmidt, M.; Baumgartl, B.; Wegner, G. *J. Phys. (Paris)* **1988**, *49*, 861–880.

(29) Xu, R. L.; Chu, B. *Macromolecules* **1989**, *22*, 3153–3161.

(30) Xu, R. L.; Chu, B. *Macromolecules* **1989**, *22*, 4523–4528.

(31) Zacher, R. A. *J. Chem. Phys.* **1990**, *93*, 1325–1331, 2139–2145.

(32) Aime, J. P.; Bargain, F.; Fave, J. L.; Rawiso, M.; Schott, M. *J. Chem. Phys.* **1988**, *89*, 6477–6483.

(33) Pearson, D. S.; Chance, R. R.; Kiss, A. D.; Morgan, K. M.; Peiffer, D. G. *Synth. Met.* **1989**, *28*, D689.

(34) Rosenblatt, C.; Rubner, M. F. *J. Chem. Phys.* **1989**, *91*, 7896–7899.

(35) Nava, A. D.; Thakur, M.; Tonelli, A. E. *Macromolecules* **1990**, *23*, 3055–3063.

(36) Chu, B.; Xu, R.; Li, Y.; Wu, D. W. *Macromolecules* **1989**, *22*, 3819–3821.

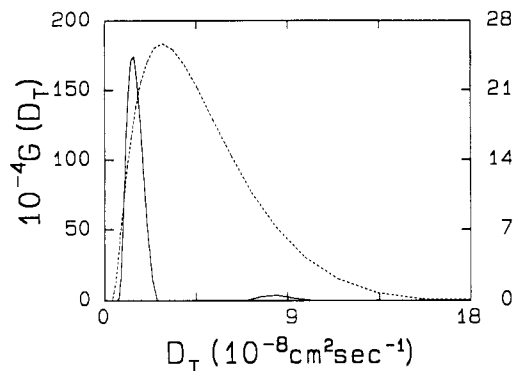


**Figure 2.** Distributions of translational diffusion coefficient ( $D_T$ ) obtained from CONTIN fittings of intensity time correlation functions of the same P4BCMU sample as in Figure 1, measured by DLS: (dashed line)  $X_c = 1.0$ ,  $C = 1.2 \times 10^{-4}$  g/g,  $K^2 = 2.82 \times 10^9$  cm $^2$  ( $\theta = 25^\circ$ ), and the right ordinate,  $\bar{D}_T = 4.9 \times 10^{-8}$  cm $^2$  s $^{-1}$  and Var = 0.34; (solid line)  $X_c = 0$ ,  $C = 1.0 \times 10^{-6}$  g/g,  $K^2 = 2.64 \times 10^9$  cm $^{-1}$  ( $\theta = 20^\circ$ ), and the left ordinate,  $\bar{D}_T = 1.5 \times 10^{-8}$  cm $^2$  s $^{-1}$  and Var = 0.04, with the small hump (only 3% in total area) ignored.  $K$  is the scattering vector. Reprinted with permission from ref 29. Copyright 1989 American Chemical Society.

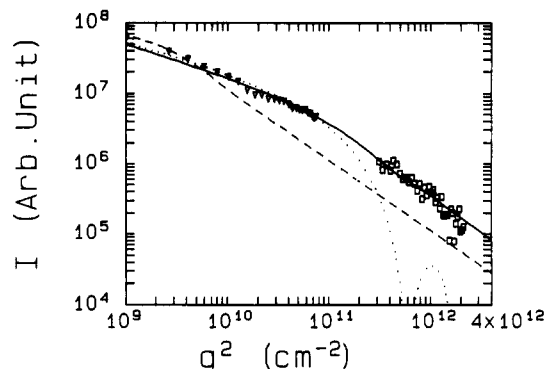


**Figure 3.** Excess scattered intensity from laser light scattering (hollow inverted triangles, measured at  $\lambda_0 = 632.8$  nm,  $C \sim 1 \times 10^{-6}$  g/g) and SAXS (hollow squares, measured at  $\lambda_0 = 0.154$  nm,  $C \sim 6 \times 10^{-6}$  g/g) for P4BCMU in dilute toluene solution at room temperatures ( $\sim 24$  °C). The three curves represent the theoretical simulations according to various models. Solid line: 14 parallel rods in a  $1 \text{ row} \times 14 \text{ column}$  configuration with the effective diameter of each individual rod being 4 nm and the effective center-to-center distance being 7 nm. Dashed line: an infinitely thin circular disk. Dotted line: a single rod, with the diameter being 100 nm. The lengths (diameters) of the rod (disk) aggregates were determined by using light-scattering and TEB results based on a rigid-rod model.<sup>29</sup>  $q$  ( $\equiv K$ ) is the scattering vector. Reprinted with permission from ref 36. Copyright 1989 American Chemical Society.

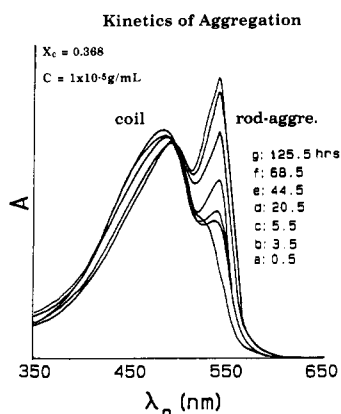


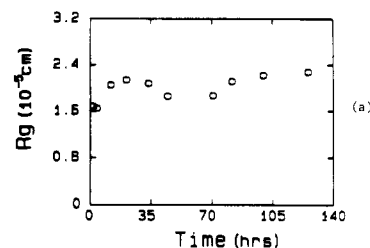
**Figure 4.** Absorption spectra as a function of time. The ordinate (absorbance  $A$ ) is in arbitrary units. The times, as indicated in labels (a-g), are from bottom up with respect to the right absorption peak. Reprinted with permission from ref 38. Copyright 1989 Hirokawa Publishing Co.

**Table II**  
**Light Scattering and TEB Results of P4BCMU Solutions<sup>a,b</sup>**

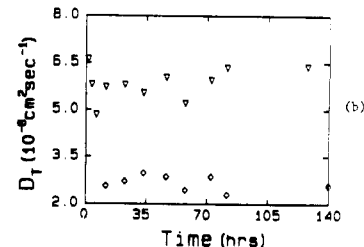
	1.2	1.2	24	24
$M_w$ ( $10^5$ g/mol)	1.2	1.2	24	24
solvent	toluene	$\text{CHCl}_3$	toluene	$\text{CHCl}_3$
color	red	yellow	red	yellow
$D_T$ ( $10^{-8}$ cm $^2$ /s)	2.14	23.8	1.84	4.87
$D_r$ (s $^{-1}$ )	24.5	—	14.5	—
Var	0.04	0.31	0.04	0.34
$R_g$ (10nm)	23	2.5	27	12
$R_h$ (10nm)	19	1.7	22	8.4
$R_{vv}^0(X_c)/R_{vv}^0(X_c=1)$	1430	1	56	1
$R_g/R_h$	1.20	1.48	1.22	1.43

<sup>a</sup>Reference 29. <sup>b</sup>Notations:  $D_T$ , rotational diffusion coefficient;  $R_g$ , radius of gyration;  $R_h$ , hydrodynamic radius;  $M_w$ , weight-average molecular weight;  $R_{vv}^0$ , Rayleigh ratio for vertically polarized incident and scattered light after extrapolation to infinite dilution and zero scattering angle.  $R_{vv}^0 \propto (\partial n/\partial C)_{T,P}^2 C M_w$  with  $(\partial n/\partial C)_{T,P}$ ,  $C$ , and  $M_w$  being the refractive index increment, the polymer (aggregate) concentration, and the weight-average molecular weight, respectively.

**Small Angle  
Light Scattering  
(PDA 20 - 27 °)**



**Dynamic  
Light Scattering  
(3rd-order CUMFIT)**



**TEB**

$X_c = 0.368$   
 $\text{CHCl}_3 / \text{toluene}$

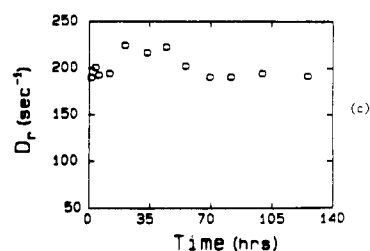


**Figure 5.** Plots of intensive properties as a function of time. The intensive properties, such as the radius of gyration ( $R_g$ ) from small angle static light scattering (SLS), the translational diffusion coefficient ( $D_T$ ) from dynamic light scattering (DLS), and the rotational diffusion coefficient ( $D_r$ ) from transient electric birefringence (TEB), show that the size and shape of the aggregates are relatively constant over a time period of about 1 week when more aggregates are being formed (see Figure 6).

tral wormlike coils of small overall size with a fairly broad size distribution. P4BCMU in a poor solvent forms charged rod-like aggregates with a narrow particle-size distribution. The techniques used in achieving this conclusion are SLS, DLS, TEB, ABS, and EP. SLS measures the angular distribution of scattered intensity as a function of concentration. From the interference effect, the  $z$ -average radius of gyration can be determined at infinite dilution. The absolute scattered in-

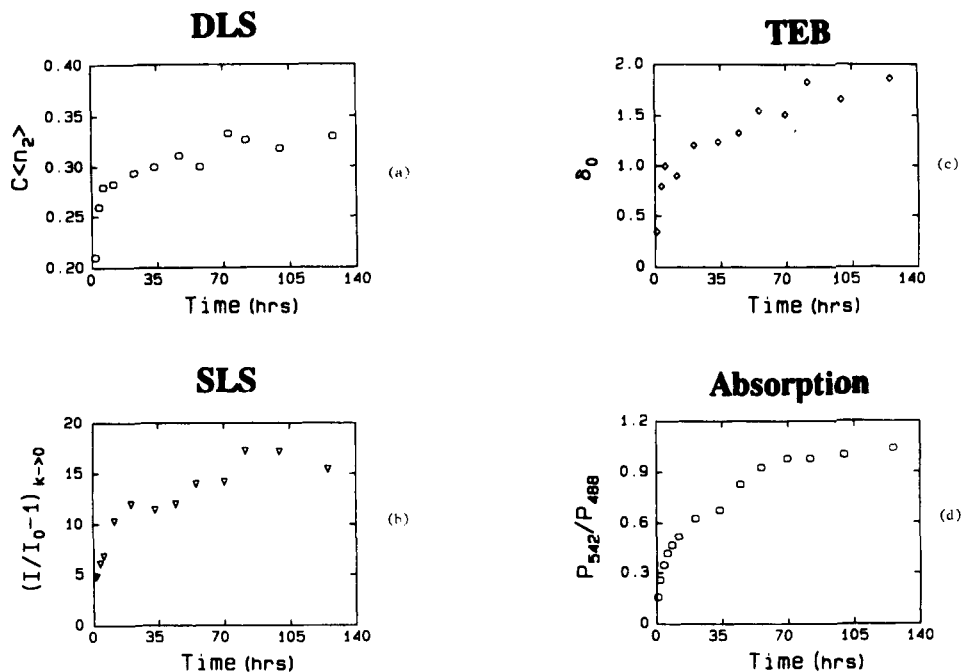


**Figure 6.** Plots of extensive properties as a function of time. The extensive properties can be related to the amount of aggregates.  $C\langle n_2 \rangle$  denotes the relative scattered intensity contributed by the aggregates as determined in a photon correlation DLS experiment.  $I/I_0$  is the ratio of scattered intensity of the solution ( $I$ ) to that of the solvent ( $I_0$ ).  $(I/I_0 - 1)_{K \rightarrow 0}$  is proportional to  $(\partial n/\partial C)_{T,P}^2 C M_w$  with  $(\partial n/\partial C)_{T,P}$ ,  $C$ , and  $M_w$  being the refractive index increment, the polymer concentration, and the weight-averaged molecular weight, respectively. If  $(\partial n/\partial C)_{T,P}$  and  $M_w$  remain relatively constant, an increase in  $(I/I_0 - 1)_{K \rightarrow 0}$  suggests an increase in the concentration of the aggregates.  $\delta_0$  represents the overall average optical anisotropy of the solution. Again, in the absence of shape changes, the magnitude of  $\delta_0$  is proportional to the amount of aggregates.  $P_{542}/P_{488}$  is the ratio of the absorption peak intensity for the coil conformation ( $\lambda_0 = 488$  nm) and the rod conformation ( $\lambda_0 = 542$  nm).

tensity after extrapolation to zero scattering angle and infinite dilution can be related to the square of the refractive index increment  $(\partial n/\partial C)_{T,P}$  of the polymer solution, the polymer concentration ( $C$ ), and the weight-average molecular weight ( $M_w$ ). As SLS emphasizes the scattering by large particles, the technique is very sensitive to the presence of even a very small amount of aggregates.

In DLS, the time dependence of the scattered intensity,  $I(t)$ , can be related to the translational (and internal) motions of the unassociated polymer molecules and the aggregates responsible for the scattered intensity. The self-beating method in photon correlation spectroscopy simply lets the scattered light mix optically within the same coherence area without the use of a reference signal from the incident laser beam. In TEB experiments, linearly polarized light is applied to a system of anisotropic particles (partially) aligned by an external electric field. The depolarized transmitted light intensity is then recorded as a function of time when the oriented anisotropic particles are relaxed back to random orientations after removal of the applied electric field. By observing the time dependence on the average orientation of anisotropic particles, the rotational diffusion coefficient ( $D_r$ ) of anisotropic particles can be determined.

The intensity time correlation function  $G^{(2)}(\tau)$  from the self-beating method in DLS has the form

$$G^{(2)}(\tau) = \langle I(t) I(t + \tau) \rangle = A \left( 1 + b \int_0^\infty G(\Gamma) e^{-\Gamma \tau} d\Gamma \right)^2 \quad (1)$$

where the bracket denotes a time-average quantity and  $I(t)$  is the scattered intensity at time  $t$ . The quantities

$A$ ,  $b$ ,  $\tau$ ,  $\Gamma$ , and  $G(\Gamma)$  are, respectively, the background, a coherence factor, the delay time, the characteristic line width, and the normalized characteristic line width distribution. From  $G^{(2)}(\tau)$ , we can then obtain information on the characteristic time  $\tau_c$  ( $\equiv \Gamma^{-1}$ ) of the system.

At small scattering angles, the characteristic line width measures the translational diffusion coefficient  $D_T$  with  $\Gamma = D_T K^2$  and  $K$  being the magnitude of the scattering vector.  $G(\Gamma)$  can be determined by Laplace inversion, a delicate transformation achievable under appropriate conditions. The polydispersity effect can be expressed in terms of the variance ( $\text{Var} = \mu_2/\bar{\Gamma}^2$ ) with

$$\bar{\Gamma} = \int \Gamma G(\Gamma) d\Gamma \quad (2)$$

$$\mu_2 = \int (\Gamma - \bar{\Gamma})^2 G(\Gamma) d\Gamma \quad (3)$$

For the charged rod-like aggregates, we present the following experimental evidence. Figure 1 shows  $[G^{(2)}(\tau)/A] - 1$  for P4BCMU ( $M_w = 2.4 \times 10^6$  g/mol) in toluene at a scattering angle  $\theta$  of  $20^\circ$  and a wavelength in vacuo  $\lambda_0$  of 632.8 nm. Figure 2 shows distributions of  $D_T$  obtained from CONTIN<sup>37</sup> (a commonly used Laplace inversion software) fittings of intensity-time correlation functions of P4BCMU in pure chloroform ( $X_c = 1.0$ , dashed line) and in pure toluene ( $X_c$

(37) Provencher, S. W. *Comput. Phys. Commun.* 1982, 27, 213-227, 229-242.

(38) Chu, B.; Xu, R. *Dynamic Behavior of Macromolecules, Colloids, Liquid Crystals and Biological Systems by Optical and Electro-Optical Methods*; Watanabe, H., Ed.; Hirokawa Publishing Co.: Tokyo, 1989; Chapter 4, pp 177-184.

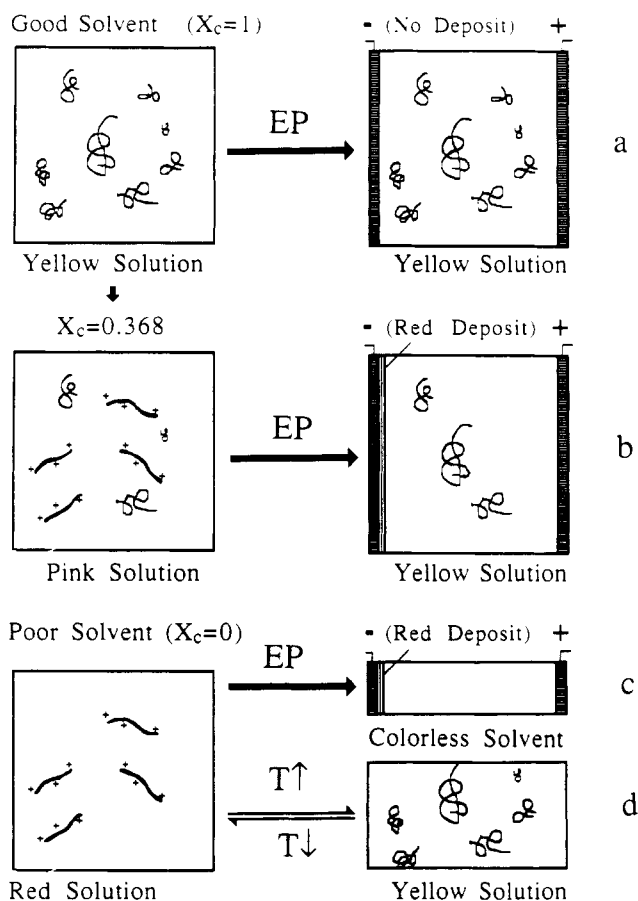


**Figure 7.** Schematics of essential features in the chromatic transition of P4BCMU. (a) Fast solubilization in good solvent ( $\text{CHCl}_3$ ). The polydisperse molecules form neutral single-chain extended coils. (b) In  $X_c = 0.368$ , coils and rod aggregates coexist. Coil sizes have been exaggerated. The rods are much larger than the coils. The slow equilibrium process takes 5 days. The red deposit can be redissolved in  $\text{CHCl}_3$  to form a yellow solution. P4BCMU in the yellow solution has a higher  $M_w$  than that of the original P4BCMU. (c) In poor solvent (toluene), the charged rod-like aggregates are relatively monodisperse. The red deposit can be redissolved in  $\text{CHCl}_3$  to form a yellow solution. (d) The transition from red solution to yellow solution can be accomplished by increasing the temperature and is very fast. The opposite process (from yellow coils to red aggregates) is slow.

$= 0$ , solid line), with  $X_c$  being the mole fraction of chloroform in the solvent. The light scattering and TEB results are listed in Table II. From the results of P4BCMU in toluene, we note that the  $D_T$ ,  $D_r$ ,  $\text{Var}$ ,  $R_g$ , and  $R_h$  values from two samples of very different molecular weights (by a factor of 10) are about the same. However, the absolute scattered intensity in terms of the Rayleigh ratio for polarized incident and scattered light after extrapolation to zero scattering angle and concentration,  $R_{90}^0 (\propto (\partial n/\partial C)_{T,P}^2 CM_w)$ , is drastically different between P4BCMU in toluene and that in chloroform, i.e.,  $R_{90}^0 (X_c = 0) \approx 1400$  and 60 times greater than  $R_{90}^0 (X_c = 1)$  for P4BCMU with  $M_w \approx 1.2 \times 10^5$  and  $2.4 \times 10^6$  g/mol, respectively. Even if the refractive index increment  $(\partial n/\partial C)_{T,P}$  value changes drastically (which is not the case) for P4BCMU in toluene and in chloroform, it cannot be used to account for all the difference between 1430 and 56 for the two P4BCMU polymers of different  $M_w$ . Thus, P4BCMU must form aggregates in toluene. The aggregates have a narrow size distribution because the  $\text{Var}$  ( $\approx 0.04$ ) value represents a near monodisperse size

distribution for both polymer samples. The aggregate size is relatively independent of the primary P4BCMU molecular weight. The  $R_h/R_g$  ( $\approx 1.2$ ) ratio suggests some form of extended chain formation. A combination of light scattering and synchrotron SAXS measurements on the structure of P4BCMU in toluene and the narrow size distribution of the aggregates as revealed by DLS permits us to model the shape of the P4BCMU aggregates as shown in Figure 3. Although we represented the structure of the P4BCMU aggregates as ribbon-like, we should not take the ribbon structure literally. The analysis suggests that the aggregated particles do not have cylindrical symmetry.<sup>39</sup> Birefringence measurements<sup>29,30</sup> further strengthen the argument for the rod-like structure. Electrophoretic separation<sup>30,31</sup> clearly demonstrates that the rod-like aggregates are charged.

For P4BCMU in a good solvent such as chloroform, we can determine the molecular weight of the *unassociated* polymer. The polymer size in terms of  $D_T$ ,  $R_g$ , and  $R_h$  now depends on  $M_w$  and differs for the two P4BCMU polymer samples of different molecular weight. The molecular weight distribution is broad with  $\text{Var} \approx 0.3$  because of the polymerization process. The  $R_g/R_h$  ratio suggests that the neutral P4BCMU coils form somewhat extended chains.

#### Time Dependence of Chromatic Transition

We used a solvent mixture of toluene and chloroform with  $X_c = 0.368$  to study the *slow* (red) color formation of P4BCMU in solution, as shown in Figure 4. The choice of  $X_c = 0.368$  is arbitrary except for the experimental convenience of slower (red) color formation. With increasing time, the first peak in Figure 4 at  $\lambda_{\text{max}1} = 438$  nm was shifted continuously to  $\lambda_{\text{max}1} = 495$  nm and the amplitude decreased, whereas the second peak position at  $\lambda_{\text{max}2} = 542$  nm remained unchanged. However, the amplitude of the second peak almost tripled during the 5-day measurement time period. Measurements of the intensive properties which are related to the structure of the aggregates show time-independent behavior, i.e.,  $R_g$  from SLS,  $\bar{D}_T$  from DLS, and  $\bar{D}_r$  from TEB show that the aggregate structure does not change as a function of time (Figure 5). On the other hand, extensive properties which are related to the amount of aggregates change as a function of time. Figure 6 shows time-dependent plots of the magnitude of optical anisotropy  $\delta_o$  from TEB, normalized peak amplitude ratio ( $P_{542}/P_{488}$ ) from ABS, excess intensity of the polymer and contrast due to the aggregate formation from DLS. The slow aggregate formation has also been observed by others.<sup>40</sup> It should be noted that, at  $X_c = 0.368$ , the coils and rod aggregates coexist at equilibrium. Analysis of the molecular weight of the coils and of the rod aggregates after electrophoretic separation showed that the rod aggregates were formed by lower molecular weight fractions of P4BCMU, in contrast to the usual polymer solution fractionation behavior. The most important point in the chromatic transition is that the formation of coils from rod aggregates is very fast. This observation agrees with magneto optic measurements.<sup>34</sup> Thus, the chromatic transitions from coils to rod aggregates

(39) Li, Y.-J.; Chu, B. *Macromolecules* 1991, 24, 4115-4122.

(40) See, for example, ref 34.

(yellow to red) and from rod aggregates to coils (red to yellow) are not entirely symmetric.

In the transition from coil to rod aggregates formation, the process can be quite slow (e.g., 5 days). The color change follows the aggregate formation as shown in Figures 5 and 6. It does not seem to be a chicken or egg type question, i.e., it is difficult to imagine that the intramolecular conformation of single polymer chains will take 5 days to equilibrate. The polymer chains can become more extended in the aggregates which take time to form. In the transition from rod aggregates to coil, the aggregates can fall apart quickly and then the more extended chains can form coils very quickly. Thus, if one heats up a red solution quickly, its change in color from red rod to yellow coil would appear to be a single-chain event after the aggregates have been broken up.

The experimental evidence obtained by a combination of physical techniques, including laser DLS and SLS, synchrotron SAXS, ABS, TEB, and EP, clearly shows single yellow coils in good solvents and red rod aggregates in poor solvents. Recent high-pressure optical absorption studies of P4BCMUs also show that the phase transition can be induced by pressure from a disordered yellow phase of coil conformation to a more ordered red phase.<sup>41</sup> The kinetics of the chromatic transition can be monitored by observing the intensive and extensive properties of the rod aggregates. The rate

(41) Variano, B. F.; Sandroft, C. J.; Baker, G. L. *Macromolecules* 1991, 24, 4376-4380.

of rod-aggregate formation varies depending upon solvent quality and temperature. At a mole fraction of chloroform of 0.368, the rod-aggregation process takes about 5 days to complete, whereas the breakup of the rod aggregates is very fast. To summarize, we provide a schematic diagram (Figure 7) which illustrates the essential features of the chromatic transition of P4BCMUs we have discussed.

One may think of an ideal experiment using a very dilute monodisperse P4BCMUs solution and ask if the single-chain chromatic transition could take place. The answer would probably be yes. However, these experiments have not been reported so far, and the conditions would be different. At extremely dilute concentrations, we can consider a single coil-to-rod transition like those observed in coil-to-globule transitions of a neutral polymer in a nonpolar solvent or of a polyelectrolyte in an aqueous solution. It is not surprising to find the aggregates to be relatively monodisperse, as in many colloidal systems. The unanswered question is, why should the P4BCMUs aggregates in solution be charged? The qualitative answers provided can certainly be improved, and a quantitative response is not yet available. Although we have emphasized our P4BCMUs results, we believe that such a chromatic transition is fairly general, applicable to other polydiacetylenes and polysilanes.

*B.C. gratefully acknowledges the support of this work by the National Science Foundation (Polymers Program, DMR8921968) and the Department of Energy (DEFG0286ER45237A005).*